RESEARCH ARTICLE

Key Points:
- Fast flows in CPS (X > −15 Re) can be classified into two classes by durations
- Substorm breakups are more closely correlated to short-duration fast flows
- Two-dimensional ion velocity distributions are different for these two fast flow classes

Correspondence to:
H. Li,
hli@spaceweather.ac.cn

Classification of fast flows in central plasma sheet: Superposed epoch analysis based on THEMIS observations

H. Li[1], C. Wang[1], and S. Y. Fu[2]

[1]State Key Laboratory of Space Weather, Center for Space Science and Applied Research, Chinese Academy of Sciences, Beijing, China, [2]Institute of Space Physics and Applied Technology, Peking University, Beijing, China

Abstract A statistical survey of 560 fast flows in midnight central plasma sheet is performed based on Time History of Events and Macroscale Interactions during Substorms (THEMIS) observations during its first two tail phases. From superposed epoch analysis, no significant substorm activities are found to be associated with the occurrence of fast flows beyond $X = −15\,Re$. Considering the associations with substorm activities, the fast flows inside of $X = −15\,Re$ can be classified into two obvious classes: short duration (< 2.0 min) and long duration (> 4.0 min). Substorm breakups are shown to be more closely correlated to short-duration fast flows. Furthermore, the onset of short-duration fast flows in the dipolarization region ($X = −9$ to $−11\,Re$) is almost simultaneous with the onset of substorm breakups and dipolarizations. On the other hand, time delays of 2–4 min are both found in the near-Earth region ($X = −7$ to $−9\,Re$) and in the near-tail region ($X = −11$ to $−15\,Re$). Assuming that short-duration fast flows are generated by the force imbalance caused by cross-tail current disruption, these features are consistent with the predictions made by the cowling electrojet current loop and the cross-tail current disruption substorm models. In comparison, although more magnetic flux is transported toward Earth for long-duration fast flows, no clear substorm breakup is closely associated with them. The analysis of 2-D ion velocity distribution further shows some differences. For short-duration fast flows, multiple crescent-shaped ion populations are found. However, for long-duration fast flows, there exists only a single crescent-shaped ion population. The difference may be an important signature for distinguishing these two classes of fast flows.

1. Introduction

Magnetotail convection is a key issue of magnetospheric study during storm/substorm, which contributes significantly to the transports of mass, energy, and magnetic flux toward Earth. The plasma flow in the magnetotail has been studied for several decades.

The average speed of plasma flows in the magnetotail is rather slow, typically below 100 km/s, both in the central plasma sheet (CPS) and the plasma sheet boundary layer (PSBL). *Huang and Frank* [1986] showed that the average plasma bulk speed in CPS is normally very low under all levels of geomagnetic activity based on the data of ISEE-1 in the first half of 1978. *Baumjohann et al.* [1989] later used 4 months of tail data obtained by Ion Release Module (IRM) onboard Active Magnetospheric Particle Tracer Explorers (AMPTE) satellite in 1986 and confirmed the findings by *Huang and Frank* [1986]. Meanwhile, *Baumjohann et al.* [1988] concluded that the average flow velocities in PSBL were surprisingly low (< 100 km/s).

In some occasions, the plasma flow in the magnetotail may be very fast and exceed several hundreds of km/s, which is first called high-speed flow by *Baumjohann et al.* [1990] and later called bursty bulk flows (BBF) by *Angelopoulos et al.* [1992]. In this study, the plasma flow in the magnetotail exceeding several hundreds of km/s is called fast flow. The fast flow events in the magnetotail were first found in PSBL in 1970s [e.g., *Lui et al.*, 1983]. *Huang and Frank* [1986] stated that fast flows rarely occur in CPS and are almost exclusively confined to PSBL. However, *Baumjohann et al.* [1990] concluded that occurrence rates of fast flow in PSBL and CPS were nearly the same. They further found that the fast flows were in bursts of typically less than 1 min duration and about 60–70% of all fast flows in CPS had a dominant component perpendicular to the magnetic field.

To explain the generation of fast plasma flows in CPS, several physical mechanisms have been proposed in the literature and have been well summarized by *Shue et al.* [2008].

1. Near-Earth magnetic reconnection mechanism [e.g., *Hones*, 1976; *Baumjohann et al.*, 1990; *Angelopoulos et al.*, 1992; *Nagai et al.*, 1998; *Machida et al.*, 1999; *Shay et al.*, 2003; *Sergeev et al.*, 2008]. Based on magnetic reconnection mechanism, magnetic energy is converted to kinetic energy. Thus, the fast flows in CPS are considered to be the outflows of magnetic reconnection.
2. The flux tube (often termed plasma bubble) mechanism [e.g., *Pontius and Wolf*, 1990; *Chen and Wolf*, 1993; *Sergeev et al.*, 1996; *Zesta et al.*, 2000; *Schödel et al.*, 2001]. The bubble may be generated by the reconnection in the far tail, as well as by other processes. A localized bubble originated in the distant tail moves earthward at high speed owing to the polarization electric fields in the bubble.
3. Force imbalance caused by the cross-tail current disruption near $X = \sim -10\ Re$ [*Lui et al.*, 1993, 2008]. *Lui et al.* [1993] have shown that cross-tail current disruption can cause a strong net force acting on the plasma, which can account for the fast flows observed near $X = \sim -10\ Re$. A typical value for the net force is 12% of its preactivity earthward $\mathbf{j} \times \mathbf{B}$ force. *Lui et al.* [2008] made an estimation of the magnitude of flow caused by cross-tail current disruption. They showed that the plasma would be accelerated to ~ 900 km/s in 15 s. Current disruption can also cause tailward flows if the net force is tailward.
4. Other possible mechanisms are the magnetic reconnection in the distant tail [*Nagai and Machida*, 1998], the retreat of near-Earth neutral line [*Baumjohann et al.*, 1999], an enhancement of large-scale ultralow frequency waves in the magnetosphere [*Lyons et al.*, 2002], and so on.

Relationships between the fast flows in CPS and the auroral activations were extensively studied in the past based on in situ observations of plasma and magnetic field in CPS and auroral images obtained by imagers on board the polar-orbit spacecraft or ground-based all-sky imagers. *Lui et al.* [1998] examined the existence of fast flows identified by the Geotail data in association with the 102 traditional substorm auroral breakups identified by the Polar UVI images and found that the fast flows were not always present during and even before the auroral breakups. *Ieda et al.* [2003] later concluded that the fast flows were more rare during the quiet intervals than at other times. However, *Shue et al.* [2003] found that about half of the earthward fast flows were associated with decreasing integrated auroral power based on Polar UVI observations, and some fast flows occurred during the period of no auroral activations. *Fairfield et al.* [1999] traced the earthward fast flows in the magnetotail observed by Geotail to the ionosphere and found that auroral brightenings developed near the foot points of fast flows. *Nakamura et al.* [2001] further concluded that all the earthward fast flows were associated with the localized auroral activations such as substorm pseudo-breakups or poleward boundary intensifications (PBI). PBIs are even expected to be an ionospheric signature of longitudinally localized earthward flow bursts [see *Rostoker et al.*, 1987; *Lyons et al.*, 2002, and references therein]. The close relationship between PBIs and flow bursts in CPS has some observational supports [see *Xing et al.*, 2010, and references therein]. Recently, the investigation of ~ 250 auroral breakup events recorded by the ground-based network of Time History of Events and Macroscale Interactions during Substorms (THEMIS) all-sky imagers revealed that auroral breakup is preceded by substantial PBIs in most cases [*Nishimura et al.*, 2010; *Mende et al.*, 2011], inferring the possibility that auroral breakup was triggered by fast flow bursts in CPS [see *Sergeev et al.*, 2012, and references therein for more details]. *McPherron et al.* [2011] found that the fast flows observed at $\sim -11\ Re$ were closely correlated with substorm onsets based on the AL index. Nevertheless, whether the fast flows in CPS are associated with the auroral brightening and further development is still under debate. For examples, *Lui et al.* [1999] showed that the near-Earth dipolarization could occur without any significant flows preceded, and *Ohtani et al.* [2002a, 2002b] suggested that the fast flows may not have a direct contribution to the substorm aurora but could create a favorable condition for a development of a substorm expansion onset.

From many previous studies, it seems possible that the fast flows could be categorized into two classes: one class is associated with the global auroral development and the other is associated with the localized auroral activations. By using the Geotail observations during 1997–1998, *Shue et al.* [2008] identified 68 earthward fast flows in the midnight CPS and found that these fast flows could be classified into two classes by their X locations. One class (Class I) of the earthward fast flows was often observed near $X = \sim -10\ Re$ with a high auroral power change rate, which suggested an apparent substorm bulge developed on the nightside, i.e., a significant global auroral development. The other class was found at $X < -15\ Re$ (Class II). For most cases of this class, the auroral power change rates were very low. The auroral features, such as PBIs and pseudo-breakups, were found to be associated with these fast flows.

As for the fast flow classification, *Shue et al.* [2008] has already obtained some interesting and important results. Nevertheless, many questions remain unanswered as elaborated below:
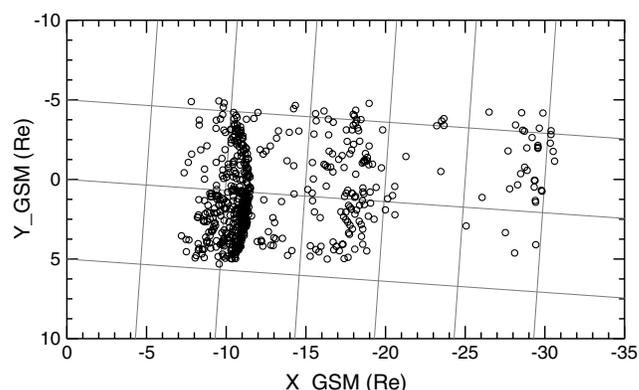
Figure 1. Distribution of fast flow locations in the equatorial plane of central plasma sheet in geocentric solar magnetospheric (GSM) coordinates. The gray grids have been rotated 4.8° clockwise to take into account the aberration due to Earth's orbital motion.

1. The number of Class I was quite few, only six events. Is this still valid for a larger database or does all the fast flow at $X = \sim -10\,Re$ belong to Class I?
2. There were still few fast flows of Class II ($\sim$10%) related to auroral bulge developments. What other property of fast flow causes that difference?
3. X location was the only criterion suggested for distinguishing these two classes of fast flows. What other property is different for these two classes of fast flows?
4. Do these two classes of fast flows have the same generation mechanism?

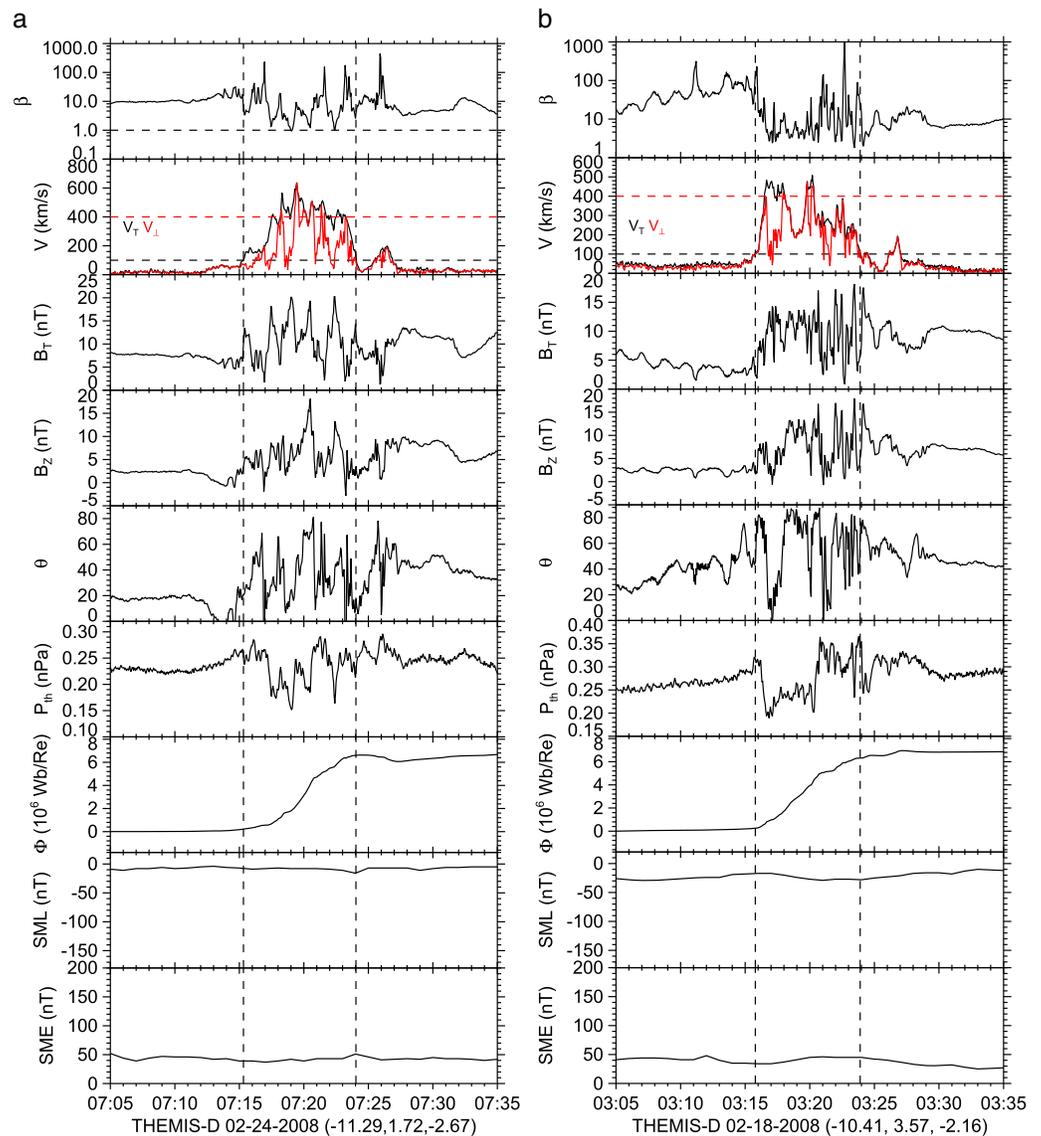The THEMIS mission with five identically instrumented probes placed in highly elliptical plane provides an excellent opportunity to extend the work of *Shue et al.* [2008] by a more comprehensive and systematic study. In an attempt to answer part of the above mentioned questions, we make a comprehensive statistical investigation of fast flow events in CPS identified by the observations of the five THEMIS probes during their first two tail phases. The rest of the paper is organized as follows: The data preparation is described in section 2, the results are presented in section 3, and the discussion and summary are given in section 4.

2. Data Preparation

The THEMIS mission was launched on 17 February 2007. It aims at resolving one of the oldest mysteries in space physics, namely to determine what physical process in near-Earth space initiates the violent eruptions of the aurora that occur during substorms in the Earth's magnetosphere. The five identically instrumented THEMIS probes are placed in highly elliptical plane. The orbit apogees for the probes are $\sim -9\,Re$ for THA; $\sim -12\,Re$ for THD and THE; $\sim -19\,Re$ for THC; and $\sim -30\,Re$ for THB.

During the first two tail phases of THEMIS mission: (1) 15 December 2007 to 15 April 2008; (2) 15 December 2008 to 15 April 2009, the five THEMIS probes were mostly in the magnetotail with their apogees sweeping the nightside region. Data from the following instruments aboard the THEMIS probes are used to identify the fast flows in CPS in this study: (1) The Flux Gate Magnetometer [*Auster et al.*, 2008], providing DC magnetic field measurements ($\sim$ 3 s, spin-fit data set); (2) The electrostatic analyzer (ESA) [*McFadden et al.*, 2008], providing ion and electron distribution functions in the energy range from 5 eV up to 25 keV for ions and from 5 eV up to 30 keV for electrons with a time resolution of a full distribution function per spin in the fast survey mode; (3) The Solid State Telescope (SST) [*Angelopoulos*, 2008], detecting high-energy ion (25 keV to 6 MeV) and electron (25 keV to 1 MeV) fluxes with a time resolution of a full distribution function per spin in the fast survey mode. By combining ESA and SST measurements, we calculated full plasma parameters, such as the plasma density, velocity, and thermal pressure.

The fast flow events in this study are first identified by an auto-search procedure by using the criterion adopted by *Angelopoulos et al.* [1992, 1994]. Then, all fast flow events are checked manually one by one. The cases with sharp density gradient which can give short-lived, spurious velocity increases are all excluded in our database. The fast flows are defined to be segments of continuous ion flow magnitude $V_T > 100$ km/s in CPS, during which V_T should exceed 400 km/s for at least two sample periods. V_T is the magnitude of the plasma flow. The fast flow begins at $V_T > 100$ km/s and ends at $V_T < 100$ km/s. If two fast flows occur within 15 min, they are considered as a continuous fast flow event. In this study, the fast flows then mentioned refer to the isolated fast flows. Similar to *Shue et al.* [2003], we also impose a criterion of plasma beta value (β) > 1.0 for covering at least 85% duration of the event on the selection of the fast flow events, where β is the ratio of the plasma thermal pressure to the magnetic pressure. This criterion ensures that THEMIS probes are mainly in CPS, not in PSBL. In addition, the criterion of β of 1.0 is to make sure that the fast flows are

Figure 2. Two fast flow events with long durations observed by THEMIS-D probe in the dipolarization region: (a) the fast flow on 24 February 2008; (b) the fast flow event on 18 February 2008. From top to bottom, the panels give the plasma β value, the flow speed (V_T) and the flow speed perpendicular to the ambient magnetic field ($V_\perp$, in red), the magnitude of magnetic field (B_T), the Z component of magnetic field (B_Z), the magnetic field elevation angle (θ) defined by $\tan^{-1}\left[B_Z = \left(B_X^2 + B_Y^2\right)\right]^{1/2}$, the thermal pressure ($P_{th}$), the cumulative magnetic flux transferred earthward/tailward and into the plasma sheet (Φ, calculated from the integration of the Y component of $\mathbf{V} \times \mathbf{B}$ over time), SML index, and SME index. Two vertical dashed lines remark the start and end of fast flows. The location of THEMIS probe in GSM coordinate system is shown in the parentheses.

mainly convective and not field aligned [*Petrukovich et al.*, 2001]. Moreover, we select events with THEMIS probes locations around the noon-midnight meridian ($| Y | \leq 5\ Re$) to avoid some magnetosheath events.

To exactly determine the substorm activity, a good direct approach is by means of the continuous auroral observation with a high time resolution from auroral imager either onboard polar-orbit satellites or equipped in the ground network. *Shue et al.* [2008] estimated the auroral power from the Polar UVI auroral images to represent substorm activity. Unfortunately, continuous aurora images are not available for most of the fast flow events. Instead, the SuperMAG auroral electrojet indices (SML and SME) calculated by *Newell and Gjerloev* [2011] are used here. The indices, SML and SME, are generalizations of the auroral electrojet indices calculated from 100 or more SuperMAG magnetometers instead of the 12 used in the official auroral electrojet indices, *AL* and *AE*. *Newell and Gjerloev* [2011] showed that the newly SuperMAG auroral electrojet
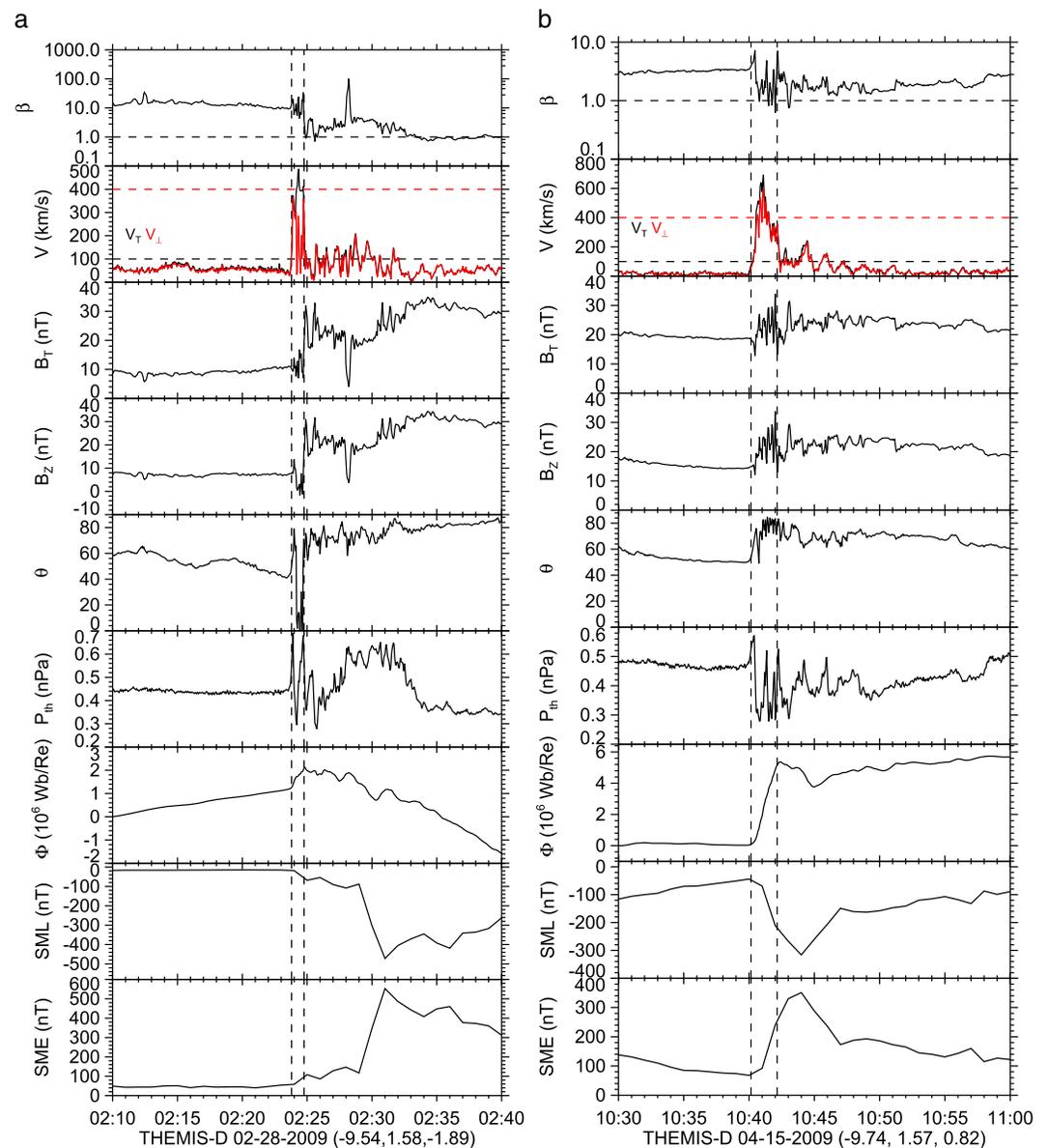
LI ET AL.   7202

Figure 3. Two fast flow events with short durations observed by THEMIS-D probe in the dipolarization region: (a) the fast flow on 28 February 2009; (b) the fast flow event on 15 April 2009. The arrangement of the plot is the same as that described in Figure 2.

indices are well correlated with the total nightside auroral power and could be used to identify substorm onsets more accurately.

3. Results

During the period of first two THEMIS scientific tail phases, 560 fast flows in CPS are identified. Note that THEMIS probes may observe the same fast flows occasionally because of their close locations, especially for THEMIS-D and THEMIS-E. In our database, some cases were observed by more than one THEMIS probe. For such cases, only the fast flows with the longest duration are included in the further analysis. The distribution of the 560 fast flows in terms of the locations in the equatorial plane of CPS is shown in Figure 1. There are significantly more fast flows inside $X = \sim -12\,Re$ because the five THEMIS probes spend more time there. Lack of events in the region at $X = -21\,Re$ to $-26\,Re$ is mainly due to the few number of times THEMIS probes being there. Remarkably, most of the events occur on the dusk side ($Y > 0$) in geocentric solar
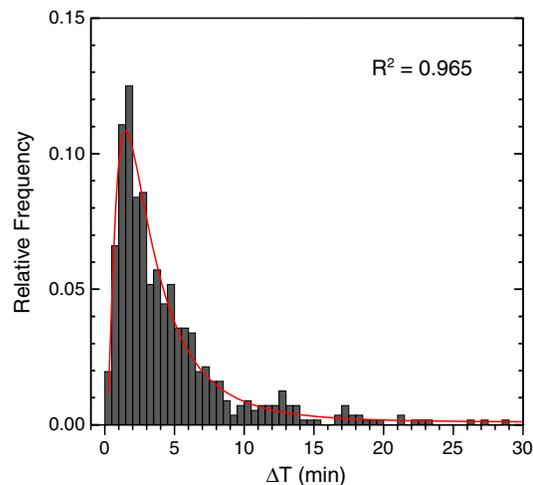
Figure 4. Histogram distribution of fast flow durations. The red line represents the fitting result to a logical normal distribution. R^2 represents the fitting goodness. The closer R^2 is to 1, the better the fitting is.

magnetospheric (GSM) coordinates, which is in consistent with the previous studies [e.g., *Angelopoulos et al.*, 1994]. This dawn-dusk asymmetry of fast flow distribution exists in the aberrated GSM coordinates as well, and about 55.0% fast flows occur on the dusk side. In addition, the percentage of fast flow occurred on the dusk side decreases as the *X* location gets far away from the Earth. For example, the percentage of fast flow occurred on the dusk side in the region with $X : -7$ to $-9\,Re$ is 77.3%. For the regions with $X : -9$ to $-11\,Re$, -11 to $-15\,Re$, and -15 to $-30\,Re$, the ratios are 64.5%, 59.2%, and 31.2%, respectively.

3.1. Comparative Cases

Among the 560 events, two classes of fast flows seem to emerge inside of $X = -15\,Re$ in CPS. However, the criterion for these two classes of fast flows is found to be their durations but not the *X* location used by *Shue et al.* [2008]. For example, two fast flows with long durations are shown in Figure 2, and two fast flows with short durations are shown in Figure 3.

Figure 2a shows the fast flow with a long duration of 8.7 min on 24 February 2008 observed by THEMIS-D at $(-11.29, 1.72, -2.67\,Re)$ in GSM coordinate system. The two vertical dashed lines represent the start (07:15:19.225 UT) and end (07:24:1.744 UT) of this fast flow event. The profile of plasma β value for this event is above the dashed horizontal line of $\beta = 1$, which implies that the fast flow occurs predominately in CPS as defined before. The flow speed perpendicular to the ambient magnetic field ($V_\perp$, in red) is bursty and comparable to the flow speed (V_T) for most of time, which suggests that fast flow is mainly convective and further confirms the suitability of the adopted selection criterion of CPS region by plasma β value. During this fast flow, the magnitude of magnetic field (B_T), its Z component (B_Z), and the thermal pressure (P_{th}) exhibit large fluctuations. Meanwhile, P_{th} is lower than the ambient plasma. Compared to preflow values, B_T, B_Z, and the magnetic field elevation angle (θ, $\tan^{-1}\left[B_Z = \left(B_X^2 + B_Y^2\right)\right]^{1/2}$) have little enhancements of ~ 4 nT, ~ 8 nT, and $\sim 20°$, respectively. These signatures indicate the occurring of a weak dipolarization process. For this long-duration fast flow, a significant cumulative magnetic flux (Φ) of 6.21×10^6 Wb/Re is transferred earthward. The cumulative magnetic flux transport per unit time per unit length is calculated from the integration of the *Y* component of the electric field in GSM coordinates over time as follows:

$$\Phi = \int E_Y \mathrm{d}t = \int (V_X B_Z - V_Z B_X)\mathrm{d}t \tag{1}$$

More details can be found in the work by *Liu et al.* [2011]. And similarly, the offset effect is also removed. It is noticed that neither the SML index nor the SME index shows any significant variation, which suggests that no substorm occurs associated with this fast flow.

Table 1. Details on the Grouping of Fast Flow Events[a]

	$X : -7$ to $-9\,Re$	$X : -9$ to $-11\,Re$	$X : -11$ to $-15\,Re$	$X : -15$ to $-30\,Re$
$\Delta T: < 2.0$ min	26 (59.1, *16.1*)	92 (41.4, *35.7*)	47 (33.6, *31.5*)	16 (10.4, *16.7*)
$\Delta T: 2.0-4.0$ min	12 (27.3, *7.8*)	74 (33.3, *30.2*)	35 (25.0, *24.6*)	34 (22.1, *37.4*)
$\Delta T: > 4.0$ min	6 (13.6, *2.1*)	56 (25.3, *12.5*)	58 (41.4, *22.5*)	104 (67.5, *62.9*)
$\overline{\Delta T}$	2.0	3.2	3.9	7.9

[a]$\overline{\Delta T}$ represents the mean value. The first number in the parentheses represents the percentage of fast flow events with different duration in the same region. The later number in italics represents the percentage of fast flow events in different regions with the same duration, and it has been normalized by the total observation time of THEMIS at these four regions in CPS.
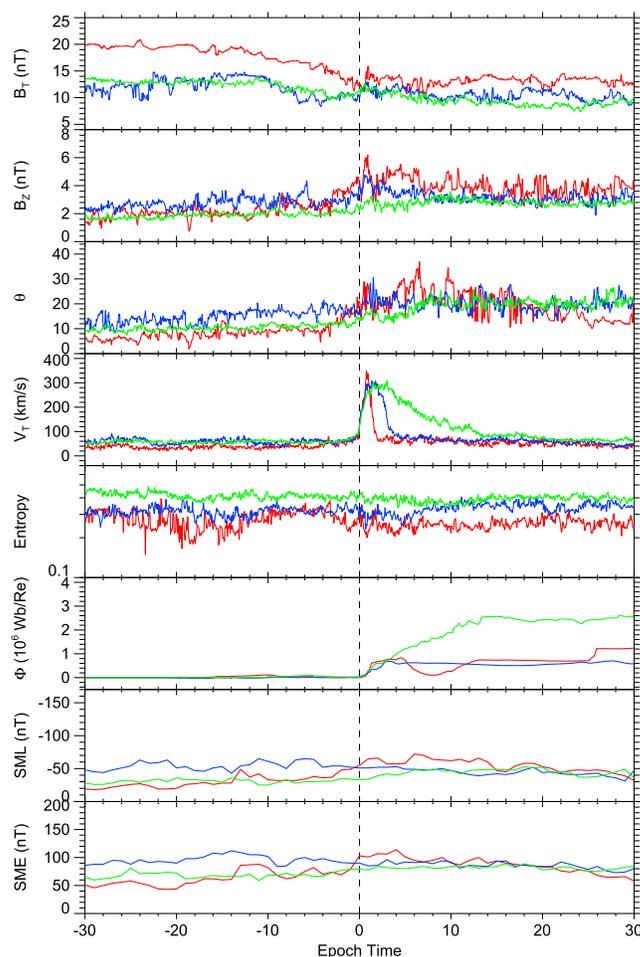
Figure 5. Results of the superposed epoch analysis for the fast flows in CPS in the midtail region. The lines in red, blue, and green represent in turn the short-duration events, moderate-duration events, and long-duration events. From top to bottom, the panels show the medians of the magnitude of magnetic field (B_T), the Z component of magnetic field (B_Z), the magnetic field elevation angle (θ), the flow speed (V_T), the entropy calculated based on the method proposed by *Wolf et al.* [2006], the cumulative magnetic flux transferred earthward (Φ), the SML index, and the SME index. The vertical dashed line represents the onset of the fast flows.

Figure 2b shows the fast flow with a long duration of 8.1 min on 18 February 2008 observed by THEMIS-D at (−10.41, 3.57, −2.16 *Re*) in GSM coordinate system. Similarly, this event also occurs in CPS, and the flow is mainly convective as well. The characters of B_T, B_Z, θ, P_{th}, and Φ are quite similar to the previous event. There exhibits a weak dipolarization after the passage of the fast flow, and the thermal pressure in the fast flow is lower than the ambient plasma. Although a significant cumulative magnetic flux of 5.96×10^6 Wb/*Re* is transferred earthward, no substorm occurs associated with this fast flow because neither the SML index nor the SME index exhibits any noticeable variation.

For comparison, Figure 3 shows two fast flows with relative short durations. Figure 3a shows the fast flow with a very short duration of 0.96 min on 28 February 2009 observed by THEMIS-D at (−9.54, 1.58, −1.89 *Re*) in GSM coordinate system. Similarly, the fast flow also occurs in CPS, with great fluctuations of B_T, B_Z, and P_{th} during its period. Moreover, B_T, B_Z, and P_{th} enhance significantly after the fast flow, by ∼ 20 nT, ∼ 20 nT, and 40°, respectively. Compared to the previous events shown in Figure 2, the dipolarization process is much stronger and lasts for longer time. Meanwhile, although the cumulative magnetic flux transferred earthward for this fast flow is much less, of only 0.61 Wb/*Re*, the SML and SME indices vary significantly right after the fast flow, indicating the development of a strong substorm.

Figure 3b shows the fast flow with a short duration of 1.99 min on 15 April 2009 observed by THEMIS-D at (−9.74, 1.57, 0.82 *Re*) in GSM coordinate system. Similarly, the fast flow also occurs in CPS, and a strong dipolarization occurs after the passage of the fast flow. The SML and SME indices vary significantly as well, indicating the development of a strong substorm.

3.2. Superposed Epoch Analysis

Different from the conclusion made by *Shue et al.* [2008], the above four typical events suggest that there seem to be two classes of fast flows in CPS inside of $X = -12\,Re$ and the substorm development seems to be more associated with short-duration fast flows. To do further confirmation, we divided all the isolated fast flow events into 12 groups, both according to their durations (ΔT) and X locations. The histogram distribution of fast flow durations is shown in Figure 4. It is close to a logical normal distribution. The peak frequency for the duration is about 2 min. The geometric mean and median values of fast flow durations are about 3 min. To make each group contain enough cases for maintaining statistical significance, the fast flows are categorized into three groups according to their durations as follows: (1) short-duration fast flows,
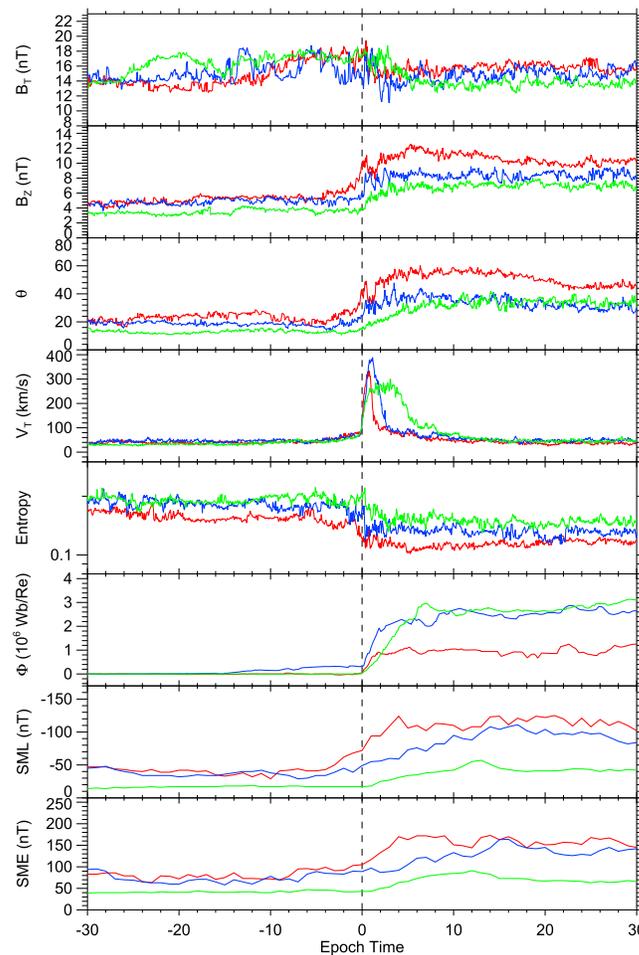
Figure 6. Results of the superposed epoch analysis for the fast flows in CPS in the near-tail region. The arrangement of the plot is the same as that described in Figure 5.

$\Delta T < 2.0$ min; (2) moderate-duration fast flows, ΔT: 2.0–4.0 min; and (3) long-duration fast flows, $\Delta T > 4.0$ min. According to the X location, the fast flows are categorized into four groups: (1) near-Earth region, X : -7 to -9 Re; (2) dipolarization region, X : -9 to -11 Re; (3) near-tail region, X : -11 to -15 Re; and (4) midtail region, X : -15 to -30 Re.

The grouping details are listed in Table 1. The mean value of ΔT decreases from 7.9 min to 2.0 min as the X location gets closer to the Earth. Meanwhile, the percentage of short-/long-duration fast flows in these four region increases/decreases accordingly, which is consistent with the popular braking scenario of fast flow in CPS [*Shiokawa et al.*, 1997]. For short-duration fast flows, they are mostly located in the dipolarization region, where the substorm-related global dipolarization processes occur. On the contrary, for long-duration fast flows, the most probable occurring region is the midtail region. Except for the group of long-duration fast flow in the near-Earth region, other groups contain enough cases for performing the superposed epoch analysis and maintaining statistical significance.

3.2.1. Superposed Epoch Analysis in Midtail Region

Figure 5 gives the comparison of superposed epoch analysis of the fast flows in the midtail region. The lines in red, blue, and green represent in turn the short-duration events, the moderate-duration events, and the long-duration events. The vertical dashed line represents the onset of the fast flows. For these three groups, B_T almost keeps invariant and the plasma entropy decreases very little after the passage of the fast flows. Meanwhile, both the SML index and the SME index keep almost invariant at quiet levels, suggesting that no significant substorm developments are associated with the fast flows in the midtail region. As *Newell and Gjerloev* [2011] proposed that the SML index and the SME index are well correlated with the total nightside auroral power, our results are consistent with the results made by *Shue et al.* [2008]. In addition, it is clear that the longer fast flow duration is, the more cumulative magnetic flux is transferred earthward ($\sim 0.4 \times 10^6$ Wb/Re, $\sim 0.6 \times 10^6$ Wb/Re, $\sim 2.6 \times 10^6$ Wb/Re, respectively). However, an interesting finding is that the signatures of a weak dipolarization (minor enhancements of B_Z and θ) are more clearly found for the short-duration events. For the moderate-duration and long-duration fast flows, B_Z and θ mostly remain their preflow values.

3.2.2. Superposed Epoch Analysis in Near-Tail Region

Figure 6 gives the comparison of superposed epoch analysis of the fast flows in the near-tail region. For these three groups of the fast flows in this region, B_T and the plasma entropy both decrease a little after the passage of the fast flows. On the contrary, enhancements of B_Z and θ are found, representing the dipolarization features. As expected, more cumulative magnetic flux is transferred earthward ($\sim 1.0 \times 10^6$ Wb/Re, $\sim 2.0 \times 10^6$ Wb/Re, and $\sim 3.0 \times 10^6$ Wb/Re, respectively) as the duration of the fast flows increases. However,
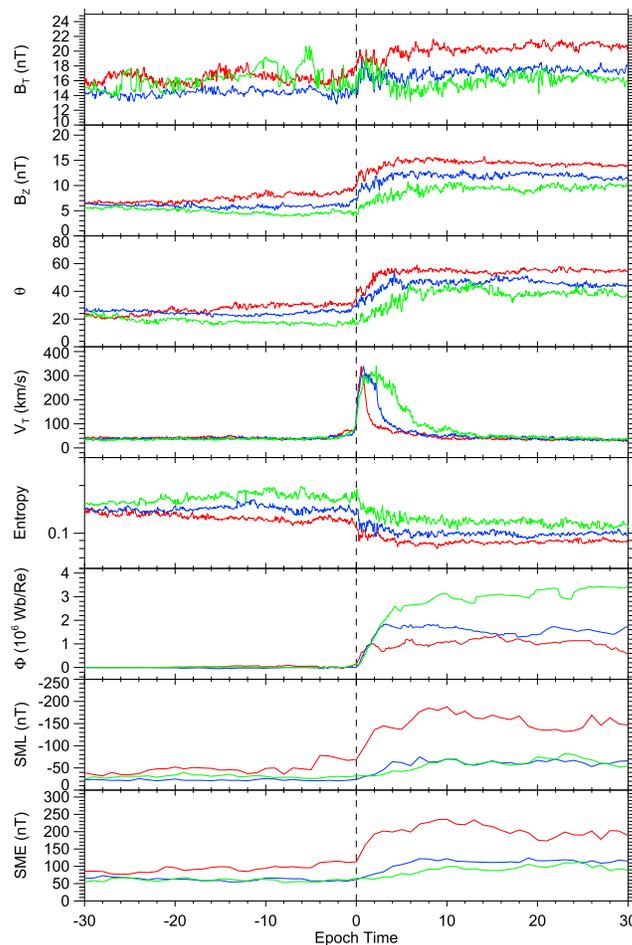
Figure 7. Results of the superposed epoch analysis for the fast flows in CPS in the dipolarization region. The arrangement of the plot is the same as that described in Figure 5.

the dipolarization intensity is larger for the short-duration events as the situation in the midtail region mentioned before. B_z enhances from ~ 5 nT to ~ 12 nT for the short-duration events, from ~ 5 nT to ~ 9 nT for the moderate-duration events, and from ~ 3.5 nT to ~ 7 nT for the long-duration events. The differences of θ change are more clear; θ enhances from $\sim 20°$ to $\sim 58°$ for short-duration events, from $\sim 16°$ to $\sim 40°$ for moderate-duration events, and from $\sim 12°$ to $\sim 36°$ for long-duration events. Note that the onset of dipolarization (both from B_z and θ) is 3–4 min earlier than the onset of fast flow for the short-duration events. For the other two groups, the onset of dipolarization is nearly simultaneous with the onset of the fast flows. The changing characteristics of the SML index and the SME index for these three groups are quite similar to those of dipolarization features:

1. The response magnitudes of the SML index and the SME index are larger as the duration of the fast flows gets shorter. The SML index decreases from -40 nT to -120 nT, from -40 nT to -100 nT, and from -15 nT to -50 nT, respectively. The SME index increases from 90 nT to 170 nT, from 90 nT to 140 nT, and from 40 nT to 80 nT, respectively.

2. The onsets of the SML index and the SME index are also 3–4 min earlier than the onset of the fast flows for the short-duration events. Compared to the moderate-duration and long-duration events, the response time of the SML index and the SME index for the short-duration events is shorter. These two indices reach their peak values 4 minutes after the onset of the fast flows. For the other two groups, the response times are 14 min and 12 min, respectively. Interestingly, the short-duration fast flows are more correlated with the substorm activities.

3.2.3. Superposed Epoch Analysis in Dipolarization Region

The comparison of superposed epoch analysis of the fast flows in the dipolarization region is given in Figure 7. For these three groups of the fast flows in this region, the plasma entropy decreases a little after the passage of the fast flows. On the contrary, B_T, B_z, and θ all increase after the passage of the fast flows, representing the dipolarization features. The shorter duration of the fast flows is, the larger preflow and post flow values for B_z and θ are. Similar to the situations in the near-tail region, more cumulative magnetic flux is transferred earthward ($\sim 1.0 \times 10^6$ Wb/Re, $\sim 2.0 \times 10^6$ Wb/Re, and $\sim 3.0 \times 10^6$ Wb/Re, respectively) as the duration of the fast flows increases. Besides, the short-duration fast flows are more correlated with the substorm activities. The response magnitudes of the SML index and the SME index are larger as the duration of the fast flows gets shorter. The SML index decreases from -70 nT to -170 nT, from -30 nT to -60 nT, and from -30 nT to -60 nT, respectively. The SME index increases from 100 nT to 220 nT, from 60 nT to 110 nT, and from 60 nT to 100 nT, respectively. Different from the short-duration events in the near-tail region, the onsets of the SML index and the SME index are almost simultaneously with the onset of the fast flows.
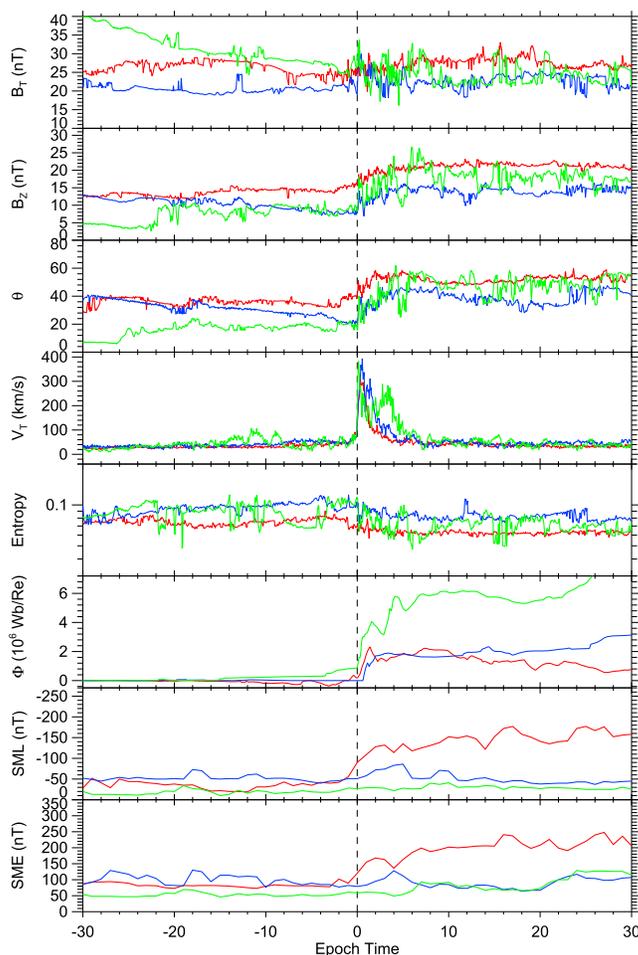
Figure 8. Results of the superposed epoch analysis for the fast flows in CPS in the near-Earth region. The arrangement of the plot is the same as that described in Figure 5.
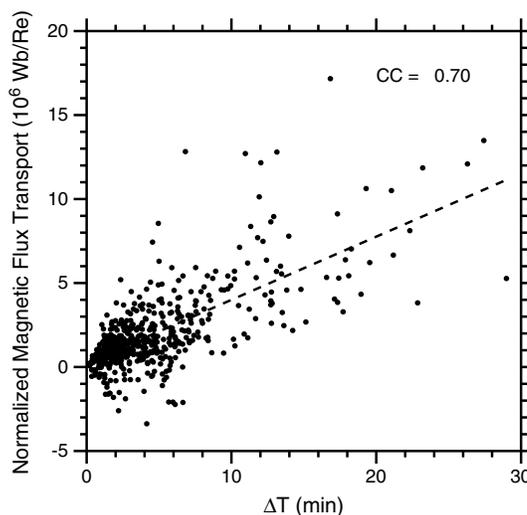

Figure 9. Relationship between the fast flow duration and cumulative magnetic flux transport to the Earth in CPS. CC represents the linear correlation coefficient.

3.2.4. Superposed Epoch Analysis in Near-Earth Region

Figure 8 gives the comparison of superposed epoch analysis of the fast flows in the near-Earth region. For these three groups of the fast flows in this region, dipolarization features and the plasma entropy decreases are similar to the situations in the dipolarization region. More cumulative magnetic flux is transferred earthward ($\sim 1.0 \times 10^6$ Wb/Re, $\sim 1.8 \times 10^6$ Wb/Re, and $\sim 3.0 \times 10^6$ Wb/Re, respectively) as the duration of the fast flows increases. The SML index and the SME index changes represent a substorm activity for the short-duration fast flow events. They change from −50 nT to −150 nT and from 90 nT to 200 nT. For other two groups, no significant variations of these two indices are found. Note that, the onsets of the SML index and the SME index are ~ 2–3 min earlier than the onset of the fast flows, which is similar to the situation in the near-tail region.

3.3. Relations Between Substorm and Fast Flows

The fast flows in CPS are believed to be the major contributor on the magnetic flux transport to the Earth. In general, the longer duration and larger earthward velocity are, the more cumulative magnetic flux is transferred earthward. Figure 9 shows the relationship between the fast flow duration and the magnetic flux transport. The magnetic flux transport is normalized by the averaged fast flow velocity perpendicular to the ambient magnetic field. As expected, there is a linear correlation between the fast flow duration and magnetic flux transport. The linear correlation coefficient is as high as 0.70.

From the perspective of median value, the previous superposed epoch analyses have suggested that the stronger substorm activity is more likely to be associated with a shorter-duration fast flow in CPS inside of $X = -15\ Re$, which is independent of the cumulative magnetic
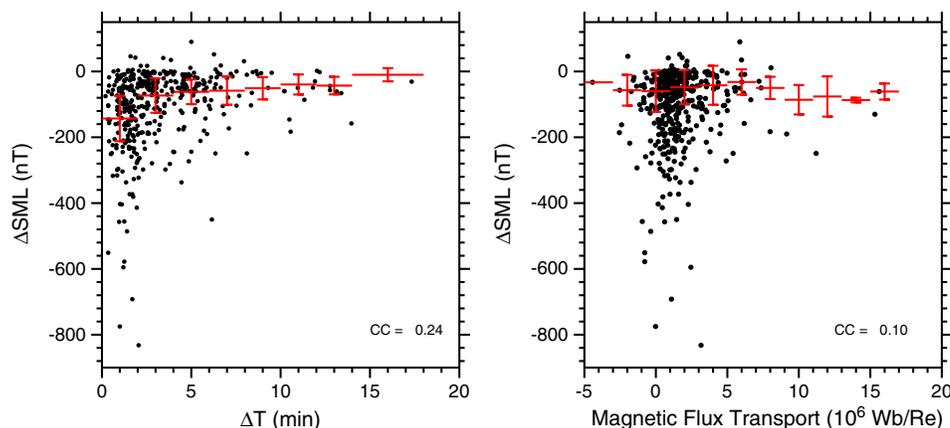
Figure 10. (left) Relationship between the intensity of substorm activity and the duration of fast flows inside $X = -15\,Re$. (right) Relationship between the intensity of substorm activity and cumulative magnetic flux transport to the Earth by the fast flows inside $X = -15\,Re$. The red horizontal line represents the mean value for each bin. The red vertical line represents the data variations, $\pm 0.5\sigma$ (standard deviation). CC represents the linear correlation coefficient.

flux transport toward the Earth. Figure 10 gives more details for each case. The difference of SML index after the passage of fast flow, ΔSML, is used to represent the intensity of substorm activity. Although the linear relationship between ΔSML and ΔT is poor, a trend is clear that stronger substorm activity tends to be associated with shorter-duration fast flows as represented by the red horizontal lines. For the strong substorm activities with ΔSML < -400 nT, the corresponding fast flow durations are mostly less than 2.5 min. For the fast flows with $\Delta T > 10$ min, the corresponding substorm activity is no stronger than that with ΔSML < -200 nT. The shown detailed relationship between ΔSML and cumulative magnetic flux transport further confirms that the intensity of substorm activity is independent of the cumulative magnetic flux transport toward the Earth. The linear correlation coefficient is only 0.10, and no clear trend is found.

Figure 11 shows the comparison of the distribution of flow duration in the region with X between $-7\,Re$ and $-15\,Re$ for different levels of substorm activity. The left panel is for intense substorm activity with ΔSML < -200 nT, and the right one is for mild substorm activity with ΔSML ≥ -200 nT. The difference is significant. For intense substorm activity situations, the distribution is more concentrated to short durations. About 70% cases are associated with short-duration fast flow. For mild substorm activity situations, the distribution is scattered to a much wider range. Only about 34% cases are associated with short-duration fast flow.
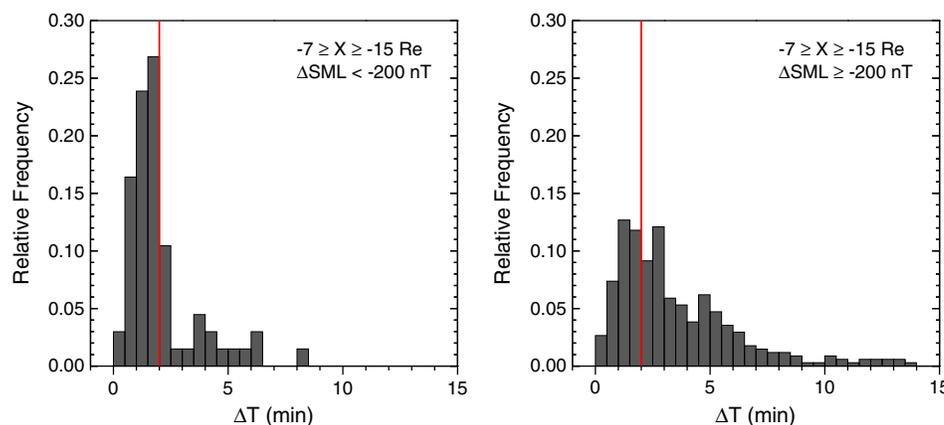

Figure 11. Comparison of the distribution of flow duration in the region with X between $-7\,Re$ and $-15\,Re$ for different levels of substorm activity. The red vertical line represents the fast flow duration of 2 min.
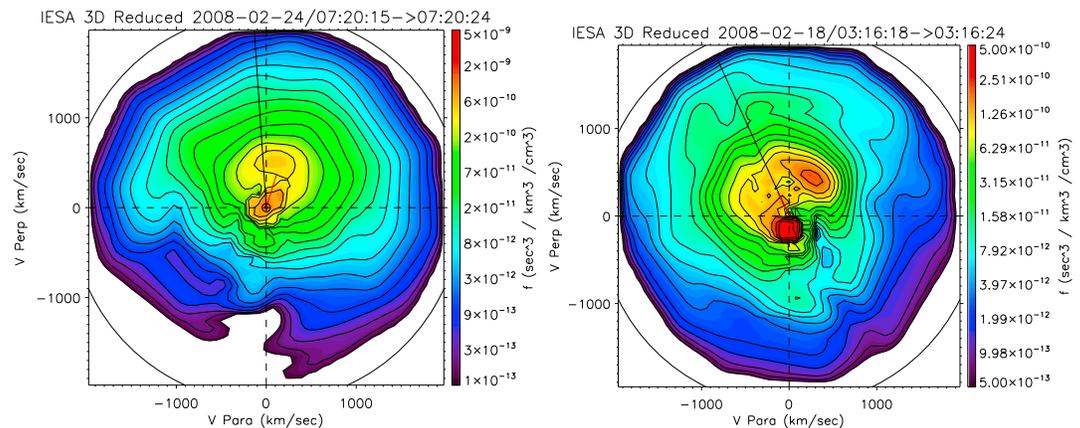
Figure 12. Velocity distribution in $V_\perp$–$V_\parallel$ plane for the fast flows with long durations. (left) The fast flow event on 24 February 2008; (right) the fast flow event on 18 February 2008.

4. Discussion and Summary

Many previous studies proposed that the fast flows in CPS brake when they move toward the Earth due to the rising magnetic field and plasma pressure, and they can link to most substorm phenomena such as dipolarization, cross-tail current disruption, and aurora activities [*Shiokawa et al.*, 1997; *Baumjohann*, 2002; *Kepko et al.*, 2001; *Nakamura et al.*, 2001; *Slavin et al.*, 2002; *Amm and Kauristie*, 2002; *Grocott et al.*, 2004; *Cao et al.*, 2008]. If the fast flow in CPS is generated by the magnetic reconnection in the magnetotail, a natural thought is that the stronger fast flow in CPS would cause stronger dipolarization and substorm intensity. Meanwhile, the pileup of magnetic flux would cause the tailward movement of the brake point of fast flows, which also means that the onset of fast flow should gradually fall behind the onset of substorm activity when the observing location moves tailward. However, the previous results show that the substorm intensity seems to be independent of the strength of short-duration fast flows. Moreover, the onset of short-duration fast flow seems to be simultaneous with the onset of substorm activity in the dipolarization region, and there is a 2–4 min time delay both in the near-Earth region and near-tail region. Compared to the near-Earth neutral line [*Shiokawa et al.*, 1998] substorm model, the CECL (cowling electrojet current loop) [*Kan et al.*, 2011] and the CD (cross-tail current disruption) [*Lui et al.*, 1991] substorm models are more suitable to interpret this phenomenon. For the CECL and CD substorm models, the force imbalance due to the cross-tail current disruption can generate short-duration fast flows in CPS, and the current disruption region can move both earthward and tailward. It is also consistent with the result that the percentage of short-duration fast flow is highest in the dipolarization region.

To check up whether there exists other different features of fast flows inside of $X = -15\,Re$, analyses of 2-D ion velocity distribution in $V_\perp$–$V_\parallel$ plane are performed for the four previous individual cases of these two classes. The results for long-duration fast flows are shown in Figure 12. For the long-duration fast flow event on 24 February 2008 and on 18 February 2008, it is clear that there exists only a single crescent-shaped ion population, and the major velocity component is perpendicular to the ambient magnetic field. The results for short-duration fast flows are shown in Figure 13. For the short-duration fast flow event on 28 February 2009 and on 15 April 2009, multiple crescent-shaped ion populations, both perpendicular component and parallel component, are found. This difference in signature may be another criterion for distinguishing these two classes of fast flows. *Raj et al.* [2002] have shown the difference of ion distribution characteristics between the high-speed bulk flows and field-aligned beams. The ion distributions of field-aligned beam usually consist mainly of earthward and tailward directed crescent-shaped beams, having sharp low-energy cutoffs, whereas high-speed bulk flows are well represented by a single drifting distribution without low-energy cutoffs. As shown in Figures 12 and 13, no sharp cutoffs in low energies are found for either long-duration fast flows or short-duration fast flows, implying that they are not field-aligned beams. In addition, multiple ion populations, not just a single ion population, are found here, which is different from *Raj et al.*'s [2002] results. Also, the ion population type is further suggested to be dependent on the duration of fast flow. More detailed statistical study about the differences of ion distribution functions needs to be conducted in the future.
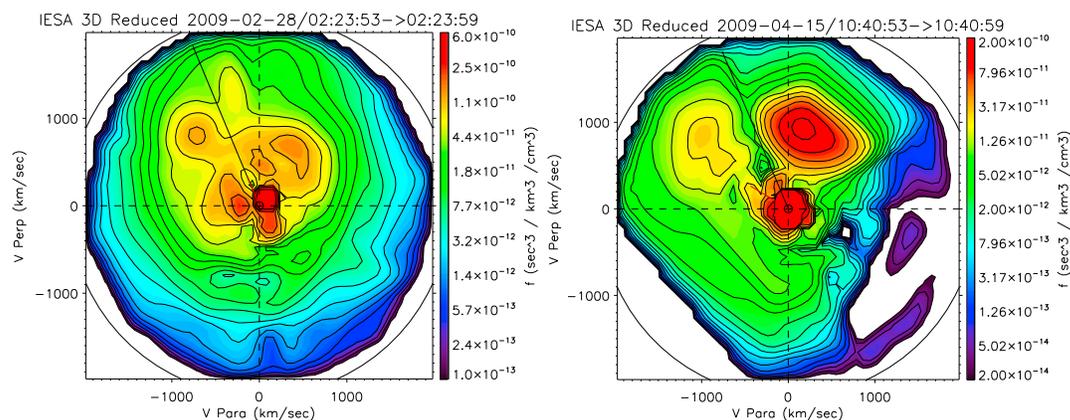
Figure 13. Velocity distribution in $V_\perp - V_\parallel$ plane for the fast flows with short durations. (left) The fast flow event on 28 February 2009; (right) the fast flow event on 15 April 2009.

In addition, we reidentify the fast flow events by using the selection criteria proposed by *Raj et al.* [2002] (perpendicular flow speed should be greater than 250 km/s, plasma β_{xy} based on the X and Y components of the magnetic field should be larger than 2.0) and repeat the previous analysis. Similar conclusions are reached.

In summary, in this study we performed a statistical survey of 560 fast flows in the midnight CPS observed by the five THEMIS probes. From superposed epoch analysis, no significant substorm activities are found to be associated with the occurrence of the fast flows beyond $X = -15\ Re$. The fast flows between $X = -7\ Re$ and $X = -15\ Re$ could be classified into two obvious classes according to their different substorm associations: one class with short duration (< 2.0 min) and the other class with a relatively longer duration (> 4.0 min). It is found that the substorm breakups are more likely to be associated with short-duration fast flows. Furthermore, the onset of short-duration fast flows in the dipolarization region is almost simultaneous with the onset of substorm breakups and dipolarizations. On the other hand, a time delay of 2–4 min are found both in the near-Earth region and in the near-tail region. Assuming that short-duration fast flows are generated by the force imbalance caused by cross-tail current disruption, these features are consistent with the predictions made by the CECL and the CD substorm models. Compared to short-duration fast flows, although more magnetic flux is transported toward Earth for long-duration fast flows, no substorm breakup is closely associated. The analysis of 2-D ion velocity distribution in $V_\perp - V_\parallel$ plane are performed for four individual cases. For the fast flows with a short duration, multiple crescent-shaped ion populations are found. However, for the cases with a long duration, there exists only a single crescent-shaped ion population. This difference may be an important signature for distinguishing these two classes of fast flows.

References

Amm, O., and K. Kauristie (2002), Ionospheric signatures of bursty bulk flows, *Surv. Geophys.*, 23, 1–32.
Angelopoulos, V. (2008), The THEMIS mission, *Space Sci. Rev.*, 141, 5–34, doi:10.1007/s11214-008-9336-1.
Angelopoulos, V., W. Baumjohann, C. F. Kennel, F. V. Coroniti, M. G. Kivelson, R. Pellat, R. J. Walker, and G. Paschmann (1992), Bursty bulk flows in the inner central plasma sheet, *J. Geophys. Res.*, 97, 4027–4039.
Angelopoulos, V., C. F. Kennel, F. V. Coroniti, R. Pellat, M. G. Kivelson, R. J. Walker, C. T. Russell, W. Baumjohann, W. C. Feldman, and J. T. Gosling (1994), Statistical characteristics of bursty bulk flow events, *J. Geophys. Res.*, 99(21), 21,257–21,280.
Auster, H. U., et al. (2008), The THEMIS fluxgate magnetometer, *Space Sci. Rev.*, 141, 235–264, doi:10.1007/s11214-008-9365-9.
Baumjohann, W. (2002), Modes of convection in the magnetotail, *Phys. Plasma*, 9(9), 3665–3667.
Baumjohann, W., G. Paschmann, N. Sckopke, C. A. Cattell, and C. W. Carlson (1988), Average ion moments in the plasma sheet boundary layer, *J. Geophys. Res.*, 93, 11,507–11,520.
Baumjohann, W., G. Paschmann, and C. A. Cattell (1989), Average plasma properties in the central plasma sheet, *J. Geophys. Res.*, 94, 6597–6606.
Baumjohann, W., G. Paschmann, and H. Lühr (1990), Characteristics of high-speed ion flows in the plasma sheet, *J. Geophys. Res.*, 95, 3801–3809.
Baumjohann, W., M. Hesse, S. Kokubun, T. Mukai, T. Nagai, and A. A. Petrukovich (1999), Substorm dipolarization and recovery, *J. Geophys. Res.*, 104, 24,995–25,000.
Cao, J. B., et al. (2008), Characteristics of mid-low latitude Pi2 excited by bursty bulk flows, *J. Geophys. Res.*, 113, A07S15, doi:10.1029/2007JA012629.
Chen, C. X., and R. A. Wolf (1993), Interpretation of high-speed flows in the plasma sheet, *J. Geophys. Res.*, 98, 21,409–21,419.
Fairfield, D. H., et al. (1999), Earthward flow bursts in the inner magnetotail and their relation to auroral brightenings, AKR intensifications, geosynchronous particle injections and magnetic activity, *J. Geophys. Res.*, 104, 355–370.

Grocott, A., T. K. Yeoman, R. Nakamura, S. W. H. Cowley, H. U. Frey, H. Reme, and B. Klecker (2004), Multi-instrument observations of the ionospheric counterpart of a bursty bulk flow in the near-Earth plasma sheet, *Ann. Geophys.*, *22*(4), 1061–1075.

Hones, E. W., Jr. (1976), The magnetotail: Its generation and dissipation, in *Physics of Solar Planetary Environments*, edited by D. J. Williams, pp. 558–571, AGU, Washington, D. C.

Huang, C. Y., and L. A. Frank (1986), A statistical study of the central plasma sheet: Implications for substorms models, *Geophys. Res. Lett.*, *13*, 652–655.

Ieda, A., et al. (2003), Quiet time magnetotail plasma flow: Coordinated Polar ultraviolet images and Geotail observations, *J. Geophys. Res.*, *108*(A9), 1345, doi:10.1029/2002JA009739.

Kan, J. R., H. Li, C. Wang, H. U. Frey, M. V. Kubyshkina, A. Runov, C. J. Xiao, L. H. Lyu, and W. Sun (2011), Brightening of onset arc precedes the dipolarization onset: THEMIS observations of two events on 1 March 2008, *Ann. Geophys.*, *29*, 2045–2059, doi:10.5194/angeo-29-2045-2011.

Kepko, L., M. G. Kivelson, and K. Yumoto (2001), Flow bursts, braking, and Pi2 pulsations, *J. Geophys. Res.*, *106*, 1903–1915.

Liu, J., C. Gabrielse, V. Angelopoulos, N. A. Frissell, L. R. Lyons, J. P. McFadden, J. Bonnell, and K. H. Glassmeier (2011), Superposed epoch analysis of magnetotail flux transport during substorms observed by THEMIS, *J. Geophys. Res.*, *116*, A00I29, doi:10.1029/2010JA015886.

Lui, A. T. Y., T. E. Eastman, D. J. Williams, and L. A. Frank (1983), Observations of ion streaming during substorms, *J. Geophys. Res.*, *88*, 7753–7764.

Lui, A. T. Y., C.-I. Chang, A. Mankofsky, H. K. Wong, and D. Winske (1991), A cross-field current instability for substorm expansions, *J. Geophys. Res.*, *96*, 11,389–11,401.

Lui, A. T. Y., P. H. Yoon, and C. L. Chang (1993), Quasi-linear analysis of ion Weibel instability, *J. Geophys. Res.*, *98*, 153–164.

Lui, A. T. Y., K. Liou, P. T. Newell, C.-I. Meng, S.-I. Ohtani, T. Ogino, S. Kokubun, M. J. Brittnacher, and G. K. Parks (1998), Plasma and magnetic flux transport associated with auroral breakups, *Geophys. Res. Lett.*, *25*, 4059–4062.

Lui, A. T. Y., K. Liou, M. Nosé, S. Ohtani, D. J. Williams, T. Mukai, K. Tsuruda, and S. Kokubun (1999), Near-Earth dipolarization: Evidence for a non-MHD process, *Geophys. Res. Lett.*, *26*, 2905–2908.

Lui, A. T. Y., et al. (2008), Determination of the substorm initiation region from a major conjunction interval of THEMIS satellites, *J. Geophys. Res.*, *113*, A00C04, doi:10.1029/2008JA013424.

Lyons, L. R., E. Zesta, Y. Xu, E. R. Sánchez, J. C. Samson, G. D. Reeves, J. M. Ruohoniemi, and J. B. Sigwarth (2002), Auroral poleward boundary intensifications and tail bursty flows: A manifestation of a large-scale ULF oscillation, *J. Geophys. Res.*, *107*(A11), 1352, doi:10.1029/2001JA000242.

Machida, S., Y. Miyashita, A. Ieda, A. Nishida, T. Mukai, Y. Saito, and S. Kokubun (1999), GEOTAIL observations of flow velocity and north-south magnetic field variations in the near and mid-distant tail associated with substorm onsets, *Geophys. Res. Lett.*, *26*(6), 635–638.

McFadden, J. P., et al. (2008), The THEMIS ESA plasma instrument and in-flight calibration, *Space. Sci. Rev.*, *141*, 277–302, doi:10.1107/s11214-008-9440-2.

McPherron, R. L., T.-S. Hsu, J. Kissinger, X. Chu, and V. Angelopoulos (2011), Characteristics of plasma flows at the inner edge of the plasma sheet, *J. Geophys. Res.*, *116*, A00I33, doi:10.1029/2010JA015923.

Mende, S. B., H. U. Frey, V. Angelopoulos, and Y. Nishimura (2011), Substorm triggering by poleward boundary intensification and related equatorward propagation, *J. Geophys. Res.*, *116*, A00I31, doi:10.1029/2010JA015733.

Nagai, T., and S. Machida (1998), Magnetic reconnection in the near-Earth magnetotail, in *New Perspectives on the Earthword Magnetotail, Geophys. Monogr. Ser.*, vol. 105, edited by A. Nishida, D. N. Baker, and S. W. H. Cowley, pp. 211–224, AGU, Washington, D. C.

Nagai, T., M. Fujimoto, Y. Saito, S. Machida, T. Terasawa, R. Nakamura, T. Yamamoto, T. Mukai, A. Nishida, and S. Kokubun (1998), Structure and dynamics of magnetic reconnection for substorm onsets with Geotail observations, *J. Geophys. Res.*, *103*(A3), 4419–4440.

Nakamura, R., W. Baumjohann, M. Brittnacher, V. A. Sergeev, M. Kubyshkina, T. Mukai, and K. Liou (2001), Flow bursts and auroral activations: Onset timing and foot point location, *J. Geophys. Res.*, *106*(A6), 10,777–10,790.

Newell, P. T., and J. W. Gjerloev (2011), Evaluation of SuperMAG auroral electrojet indices as indicators of substorms and auroral power, *J. Geophys. Res.*, *116*, A12211, doi:10.1029/2011JA016779.

Nishimura, Y., L. Lyons, S. Zou, V. Angelopoulos, and S. Mende (2010), Substorm triggering by new plasma intrusion: THEMIS all-sky imager observations, *J. Geophys. Res.*, *115*, A07222, doi:10.1029/2009JA015166.

Ohtani, S., R. Yamaguchi, M. Nosé, H. Kawano, M. Engebretson, and K. Yumoto (2002a), Quiet time magnetotail dynamics and their implications for the substorm trigger, *J. Geophys. Res.*, *107*(A2), SMP 6-1–SMP 6-10, doi:10.1029/2001JA000116.

Ohtani, S., R. Yamaguchi, H. Kawano, F. Creutzberg, J. B. Sigwarth, L. A. Frank, and T. Mukai (2002b), Does the braking of the fast plasma flow trigger a substorm? A study of the August 14, 1996, event, *Geophys. Res. Lett.*, *29*, 16-1–16-4, doi:10.1029/2001GL013785.

Petrukovich, A. A., W. Baumjohann, R. Nakamura, R. Schdöel, and T. Mukai (2001), Are earthward bursty bulk flows convective or field-aligned?, *J. Geophys. Res.*, *106*, 21,211–21,215.

Pontius, D. H., Jr., and R. A. Wolf (1990), Transient flux tubes in the terrestrial magnetosphere, *Geophys. Res. Lett.*, *17*, 49–52.

Raj, A., T. Phan, R. P. Lin, and V. Angelopoulos (2002), Wind survey of high-speed bulk flows and field-aligned beams in the near-Earth plasma sheet, *J. Geophys. Res.*, *107*(A12), 1419, doi:10.1029/2001JA007547.

Rostoker, G., A. T. Y. Lui, C. D. Anger, and J. S. Murphree (1987), North-south structure in the midnight sector auroras as viewed by the VIKING imager, *Geophys. Res. Lett.*, *14*, 407–410.

Schödel, R., W. Baumjohann, R. Nakamura, V. A. Sergeev, and T. Mukai (2001), Rapid flux transport in the central plasma sheet, *J. Geophys. Res.*, *106*, 301–313.

Sergeev, V. A., V. Angelopoulos, J. Gosling, C. Cattell, and C. Russell (1996), Detection of localized, plasma-depleted flux tubes or bubbles in the midtail plasma sheet, *J. Geophys. Res.*, *101*, 10,817–10,826.

Sergeev, V., et al. (2008), Study of near-Earth reconnection events with Cluster and Double Star, *J. Geophys. Res.*, *113*, A07S36, doi:10.1029/2007JA012902.

Sergeev, V. A., V. Angelopoulos, and R. Nakamura (2012), Recent advances in understanding substorm dynamics, *Geophys. Res. Lett.*, *39*, L05101, doi:10.1029/2012GL050859.

Shay, M. A., J. F. Drake, M. Swisdak, W. Dorland, and B. N. Rogers (2003), Inherently three dimensional magnetic reconnection: A mechanism for bursty bulk flows?, *Geophys. Res. Lett.*, *30*(6), 1345, doi:10.1029/2002GL016267.

Shiokawa, K., W. Baumjohann, and G. Haerendel (1997), Braking of high-speed flows in the near-Earth tail, *Geophys. Res. Lett.*, *24*(10), 1179–1182, doi:10.1029/97GL01062.

Shiokawa, K., et al. (1998), High-speed ion flow, substorm current wedge, and multiple Pi 2 pulsations, *J. Geophys. Res.*, *103*, 4491–4507, doi:10.1029/97JA01680.

Shue, J.-H., S. Ohtani, P. T. Newell, K. Liou, C.-I. Meng, A. Ieda, and T. Mukai (2003), Quantitative relationships between plasma sheet fast flows and nightside auroral power, *J. Geophys. Res.*, *108*(A6), 1231, doi:10.1029/2002JA009794.

Shue, J.-H., A. Ieda, A. T. Y. Lui, G. K. Parks, T. Mukai, and S. Ohtani (2008), Two classes of earthward fast flows in the plasma sheet, *J. Geophys. Res.*, *113*, A02205, doi:10.1029/2007JA012456.

Slavin, J. A., et al. (2002), Simultaneous observations of earthward flow bursts and plasmoid ejection during magnetospheric substorms, *J. Geophys. Res.*, *107*(A7), SMP 13-1–SMP 13-23, doi:10.1029/2000JA003501.

Xing, X., L. Lyons, Y. Nishimura, V. Angelopoulos, D. Larson, C. Carlson, J. Bonnell, and U. Auster (2010), Substorm onset by new plasma intrusion: THEMIS spacecraft observations, *J. Geophys. Res.*, *115*, A10246, doi:10.1029/2010JA015528.

Wolf, R. A., V. Kumar, F. R. Toffoletto, G. M. Erickson, A. M. Savoie, C. X. Chen, and C. L. Lemon (2006), Estimating local plasma sheet $PV^{5/3}$ from single-spacecraft measurements, *J. Geophys. Res.*, *111*, A12218, doi:10.1029/2006JA012010.

Zesta, E., L. R. Lyons, and E. Donovan (2000), The auroral signature of earthward flow bursts observed in the magnetotail, *Geophys. Res. Lett.*, *27*, 3241–3244.